TABLE 3 Comparison of Measured Performance Parameters of the Antenna

Frequency (GHz)	3 dB Beamwidth		Sidelobe Level (dB)		Gain (dBi)
	E-Plane	*H*-Plane	*E*-Plane	*H*-Plane	
11.35	22.5°	24.0°	−12.90	−13.00	12.60
11.80	31.0°	35.5°	−13.70	−15.60	14.50
12.25	28.0°	26.0°	−14.70	−13.40	15.26
12.70	21.0°	21.5°	−13.20	−14.50	15.35
13.45	22.0°	28.0°	−8.40	−11.80	15.33
14.05	17.5°	19.5°	−9.10	−14.60	15.05

Raheel M. Hashmi is currently at CSIRO Computational Informatics, Marsfield, NSW, Australia.

compares very well with other ERAs and horn antennas. The presented ERA is simple to construct, can provide high gain in a very small lateral area and is able to support linear, dual-linear, and circular polarizations, with appropriate modifications to the feed. Its very small lateral area is a great advantage in footprint-limited point-to-point applications.

ACKNOWLEDGEMENTS

This work was supported in part by the Commonwealth of Australia IPRS (No. 2012003), AISRF, and the CSIRO Astronomy & Space Science OCE Scholarship (N01759). The authors would like to thank Rogers Inc., for providing the dielectric materials used in the antenna prototype for experiments.

REFERENCES

1. A.P. Feresidis and J.C. Vardaxoglou, High gain planar antenna using optimised partially reflective surfaces, Proc Inst Elect Eng Microwave Antennas Propag 148 (2001), 345–350.
2. C. Serier, C. Cheype, R. Chantalat, M. Thvenot, T. Mondire, A. Reineix, and B. Jecko, 1-D photonic bandgap resonator antenna, Microwave Opt Technol Lett 29 (2001), 312–315.
3. A.R. Weily, K.P. Esselle, B.C. Sanders, and T.S. Bird, High-gain 1D EBG resonator antenna, Microwave Opt Technol Lett 47 (2005), 107–114.
4. G. Lovat, P. Burghignoli, F. Capolino, and D. Jackson, Bandwidth analysis of highly-directive planar radiators based on partially-reflecting surfaces, In: European Conference on Antennas Propagation, Nice, France, 2006, pp. 1–6.
5. A.R. Weily, K.P. Esselle, T.S. Bird, and B.C. Sanders, Dual resonator 1-D EBG antenna with slot array feed for improved radiation bandwidth, IET Microwave Antennas Propag 1 (2007), 198–203.
6. G. Yuehe, K.P. Esselle, and T.S. Bird, The use of simple thin partially reflective surfaces with positive reflection phase gradients to design wideband, low-profile EBG resonator antennas, IEEE Trans Antennas Propag 60 (2012), 743–750.
7. L. Moustafa and B. Jecko, EBG structure with wide defect band for broadband cavity antenna applications, IEEE Antennas Wireless Propag Lett 7 (2008), 693–696.
8. M. Al-Tarifi, D. Anagnostou, A. Amert, and K. Whites, Bandwidth enhancement of the resonant cavity antenna by using two dielectric superstrates, IEEE Trans Antennas Propag 61 (2013), 1898–1908.
9. R.M. Hashmi, B.A. Zeb, and K.P. Esselle, Wideband high gain EBG resonator antennas with small footprints and all-dielectric superstructures, IEEE Trans Antennas Propag 62 (2014), 2970–2977.
10. M.A. Al-Tarifi, A.K. Amert, D. Anagnostou, and K.W. Whites, Application of a dielectric puck for a high gain-bandwidth resonant cavity antenna, In: IEEE International Symposium on Antennas and Propagation Society, Chicago, 2012, 1–2.
11. R.M. Hashmi, B.A. Zeb, K.P. Esselle, and S.G. Hay, Effect of truncating the superstructures in broadband Fabry-Perot cavity antennas, In: IEEE/MTT International Microwave and Optoelectronics Conference, Rio de Janeiro, Brazil, 2013.
12. D.R. Jackson, P. Burghignoli, G. Lovat, F. Capolino, C. Ji, D.R. Wilton, and A.A. Oliner, The fundamental physics of directive beaming at microwave and optical frequencies and the role of leaky waves, Proc of IEEE 99 (2011), 1780–1805.
13. T.S. Bird and C. Granet, Optimization of profiles of rectangular horns for high efficiency, IEEE Trans Antennas Propag 55 (2007), 2480–2488.
14. Z. Ma and G. Vandenbosch, Low-cost wideband microstrip arrays with high aperture efficiency, IEEE Trans Antennas Propag 60 (2012), 3028–3034.
15. N. Zhu and R. Ziolkowski, Photoconductive THz antenna designs with high radiation efficiency, high directivity, and high aperture efficiency, IEEE Trans THz Sci Technol 3 (2013), 721–730.

ON THE EQUIVALENT CIRCUIT, INPUT IMPEDANCE, REFLECTION COEFFICIENT, AND BANDWIDTH OF PRINTED MONOPOLE ANTENNA

S. Bhattacharjee, R. S. Kshetrimayum, and R. Bhattacharjee
Department of Electronics and Electrical Engineering, Indian Institute of Technology Guwahati, Guwahati 781039, India; Corresponding author: b.somen@iitg.ernet.in

Received 2 January 2015

ABSTRACT: *This article presents the derivation of a closed form expression for input admittance of horizontal electric dipole over an ungrounded substrate using transmission line analogy. The derived expression is then used to calculate reflection coefficient of rectangular and circular printed monopole antenna (PMA) fed by a microstrip line. Analytical result for the reflection coefficient of both rectangular and circular PMA is verified using high frequency structure simulator (HFSS). For circular PMA, analytical, and simulated results are also compared with the measured results available in literature. Effect of the dimension and dielectric material on the antenna bandwidth is also studied and verified by HFSS.* © 2015 Wiley Periodicals, Inc. Microwave Opt Technol Lett 57:1535–1538, 2015; View this article online at wileyonlinelibrary.com. DOI 10.1002/mop.29130

Key words: *printed monopole antenna; antenna bandwidth; antenna input impedance*

1. INTRODUCTION

Printed monopole antenna (PMA) is one of the most suitable choices for wideband and ultrawideband applications due to its large impedance bandwidth (BW) and nearly omnidirectional radiation pattern. Most of the experimental and simulation work on different PMA structure has already been done and some of them are available in the literature [1–3]. Finite difference time domain (FDTD) and characteristic mode theory-based analysis of PMA fed by CPW are available in [4,5], respectively. Electric field integral equation and method of moment analysis of printed strip monopole antenna are also presented in [6]. This article discusses the analytical evaluation of input impedance as well as reflection coefficient of rectangular and circular PMA. Analytical model of antennas provide physical insight into the antenna operation and the same helps in preliminary design of antennas, which can be refined further using different computer aided design (CAD) tools available. An analytical model of PMA using transmission line analogy provides useful information on the dependence of antenna parameters on its dimensions and substrate material. PMA is structurally similar to simple

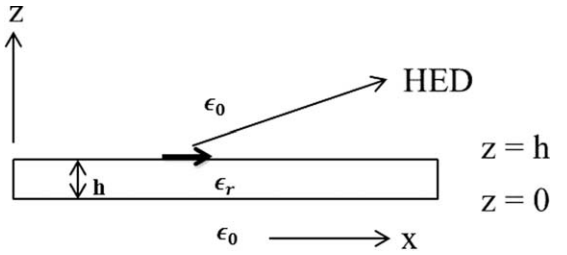

Figure 1 Geometry of HED along x-axis on the interface of dielectric and free space

microstrip antenna (MSA) with only difference that the ground plane is removed below the patch. Thus, PMA can be modelled in terms of unit horizontal electric dipole (HED) lying on a substrate which is not backed by a ground plane. Thus, transmission line analogy is an effective way to derive the closed form expressions for the input impedance and reflection coefficient of PMA. The substrate layer can be modelled as a transmission line with characteristic impedance and propagation constant depends on angle of incidence θ [7]. As the characteristic impedance also depends on the substrate material, thus, the expression for theoretical input impedance gives some physical insight on the behavior of PMA with respect to variation in ε_r and substrate thickness h. Results for the reflection coefficient evaluated from the theoretical input impedance expression of a rectangular PMA fed by 50 Ωmicrostrip line is compared with Ansoft high frequency structure simulator (HFSS) results. Reflection coefficient of a circular PMA is also evaluated using the theoretical method proposed in this article and the same is compared with simulation (HFSS) results as well as results already available in literature [8]. Dependence of impedance BW on substrate material and dimensions of the antenna is also discussed in Section 3.

2. THEORY

Assume a HED lying on a lossy and ungrounded dielectric substrate as shown in Figure 1. The input admittance Y_{in} is evaluated in the dielectric when source is in the air at an specified angles θ, ϕ in spherical coordinates. Using reciprocity theorem $Y_{in,TE}$ or $Y_{in,TM}$ is the admittance due to the source lying on the interface (between air and dielectric) seen from air for transverse electric (TE) or transverse magnetic (TM) cases. The term $Y_{in,TE}$ or $Y_{in,TM}$ depends on the angle θ. The source accounted for reciprocity on the interface can be represented by the plane wave incident on transmission line of different lengths equal to height of each dielectric layer. Figure 2 represents the wave incident from the Region 2 (air) on the dielectric at angle θ,

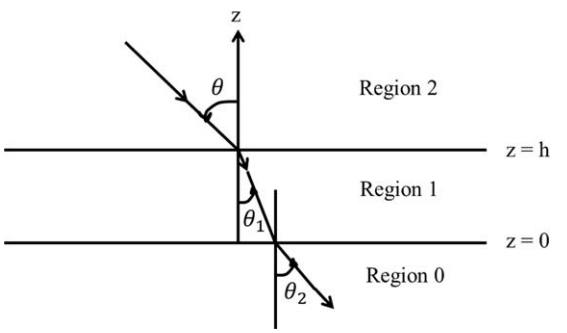

Figure 2 Equivalent wave description of printed monopole antenna

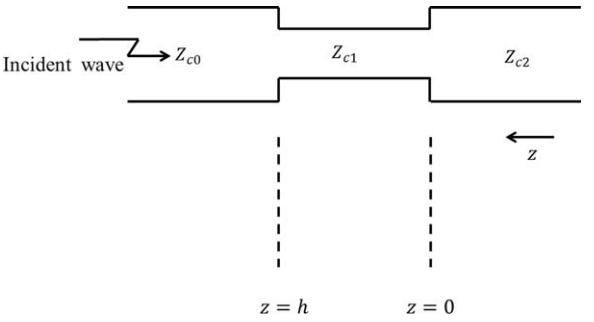

Figure 3 Transmission line model of printed monopole antenna

enters into Region 1 (dielectric) at angle θ_1, and wave emerges out to Region 0 (air) at an angle θ_2.

2.1. Transmission Line Equivalent of PMA

Here, the substrate layer is modelled as transmission line with the length equal to the substrate thickness h and propagation constant depends on angle θ [7], which terminates at the characteristic impedance of air Z_{c2}.

Now, using the equivalent transmission line model for PMA is shown in Figure 3, the input admittance for the TE polarization case can be written as

$$Y_{in,TE} = \frac{n_1(\theta)}{\eta_0}\frac{\frac{\eta_0}{n_1(\theta)} + j\eta_0\sec(\theta)\tan(\beta_1 h)}{\eta_0\sec(\theta) + j\frac{\eta_0}{n_1(\theta)}\tan(\beta_1 h)} \tag{1}$$

The above expression is input admittance of a HED on an ungrounded substrate for TE polarization case can be derived using the procedure of [7] in which characteristic impedance in air (Z_{c0} and Z_{c2}) is $\eta_0\sec(\theta)$, whereas characteristic impedance in substrate (Z_{c1}) is $\eta_0/n_1(\theta)$, $n_1(\theta)$ is the effective refraction index dependent on angle θ equal to $\sqrt{\varepsilon_r - \sin^2(\theta)}$and propagation constant $\beta_1 = k_0 n_1(\theta)$.

Similarly input admittance for TM polarization case can be written as

$$Y_{in,TM} = \frac{\varepsilon_r}{\eta_0 n_1(\theta)}\frac{\frac{\eta_0 n_1(\theta)}{\varepsilon_r} + j\eta_0\cos(\theta)\tan(\beta_1 h)}{\eta_0\cos(\theta) + j\frac{\eta_0 n_1(\theta)}{\varepsilon_r}\tan(\beta_1 h)} \tag{2}$$

In this case, characteristic impedance in air is $\eta_0\cos(\theta)$, whereas characteristic impedance in substrate is $\eta_0 n_1(\theta)/\varepsilon_r$, and rest of the parameters are same as in TE polarization case. For majority of the practical cases, PMAs have very thin substrate thickness, so for thin substrate cases, that is, when h is small and $(\theta = 0)$ (for perpendicular incidence) both Eqs. (1) and (2) becomes

$$Y_{in} = \frac{1}{\eta_0} + j\frac{k_0 h}{\eta_0}(\varepsilon_r - 1) \tag{3}$$

Now, if we replace ε_r by $\varepsilon_r(1 - j\tan(\delta))$ where $\tan(\delta)$ is very small amount of loss in the dielectric, then after some algebraic operations, (3) gives overall resistance $R = \eta_0/(1 + k_0 h\ \varepsilon_r\tan(\delta))$, capacitance $C = k_0 h(\varepsilon_r - 1)/\omega_0\eta_0$, and inductance $L = \eta_0/\omega_0 k_0 h(\varepsilon_r - 1)$, respectively.

Here, ω_0 is resonant frequency of the structure and η_0 is the free space characteristic impedance nearly equal to 377 Ω. Using the value of R, L, and C, we can evaluate the Q value for the shunt resistor-inductor-capcitor (RLC) circuit, thus, we can determine the BW of the structure shown in Figure1. Hence, BW can be expressed as

TABLE 1 Bandwidth Calculation

Substrate	1st term in (4)	2nd term in (4)
FR4 epoxy	3	0.03
RT duriod 5870	7.5	0.002
RT duriod 5880	8.3	0.001

$$\mathrm{BW} = \frac{1}{k_0 h(\varepsilon_r - 1)} + \frac{\varepsilon_r \tan(\delta)}{(\varepsilon_r - 1)} \tag{4}$$

The value of first and second term for BW expression in (4) for different substrate material of thickness $h = 1.59$ mm with operating frequency of 3 GHz are listed below in Table 1.

From Table 1, we find that the value of second term in (4) is very small compared with the first term, so we can neglect the second term. Hence, (4) can be written as

$$\mathrm{BW} \approx \frac{1}{k_0 h(\varepsilon_r - 1)} \tag{5}$$

Thus, from (5), we observe that BW is inversely proportional to ε_r. This is well-known for MSAs, but not theoretically investigated for PMAs.

3. RESULTS

The above results are limited to the HED, input impedance calculation for PMA is performed using the following equation [9]

$$Z_{\mathrm{in}} = -\frac{hI_s}{I_0}\left(\frac{1}{Y_{\mathrm{in(TE\,or\,TM)}}}\right) \tag{6}$$

where I_s is the current setup by the microstrip line feed on the antenna which is given by $I_0 \sin((x - 0.5L)/L)/W$. Thus, reflection coefficient can be effectively evaluated from input impedance of printed rectangular monopole antenna.

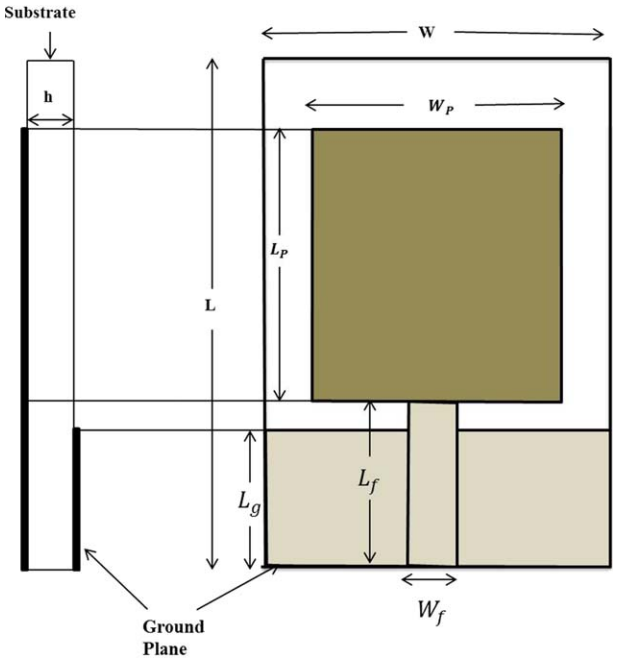

Figure 4 Geometry of a rectangular printed monopole antenna. [Color figure can be viewed in the online issue, which is available at wileyonlinelibrary.com]

TABLE 2 Detailed Dimensions

	Dimension of rectangular PMA							
Parameters	L_p	W_p	L_f	W_f	L_g	L	W	h
Units(mm)	46	42	17.8	2.96	15	76	81	1.59

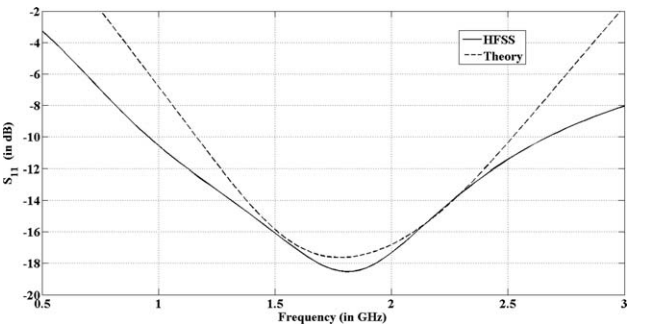

Figure 5 Plot of reflection coefficient of a rectangular printed monopole antenna in dB

The proposed technique is validated by HFSS simulation using rectangular PMA on FR4 substrate ($\varepsilon_r = 4.4$) having thickness 1.59 mm with loss tangent of 0.02 fed by a 50 Ω microstrip line. The geometry of the antenna is shown in Figure 4.

The detailed dimensions of the rectangular PMA shown in Figure 4 are listed below in Table 2. The performance of this transmission line-based approach has also been verified in case of a circular PMA [8].

3.1. Discussions

Figure 5 shows both theoretical as well simulation results of reflection coefficient (in dB) of simple rectangular PMA which is in good agreement. Equivalent surface area model of square and circular patch discussed in [10] is used to calculate reflection coefficient of printed circular PMA and the theoretical results are validated by HFSS. In Figure 6, the theoretical and HFSS results are compared with the results of circular PMA available in [8]. It may be noted that [8] provides simulation results of circular PMA computed using CST Microwave Studio as well as measured data. There is a slight difference in the simulation, analytical, and experimental results. This may be attributed to the fact that the feed gap between the patch and ground plane has been neglected in the analytical study. It is interesting to note that BW gets affected by broadening the width of the

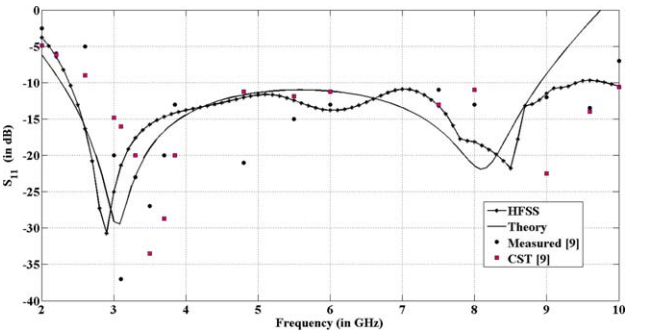

Figure 6 Plot of reflection coefficient of a circular printed monopole antenna [9] in dB. [Color figure can be viewed in the online issue, which is available at wileyonlinelibrary.com]

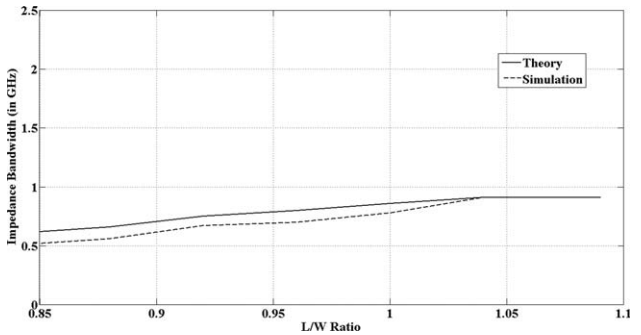

Figure 7 Variation of L/W ratio vs. impedance BW for rectangular PMA

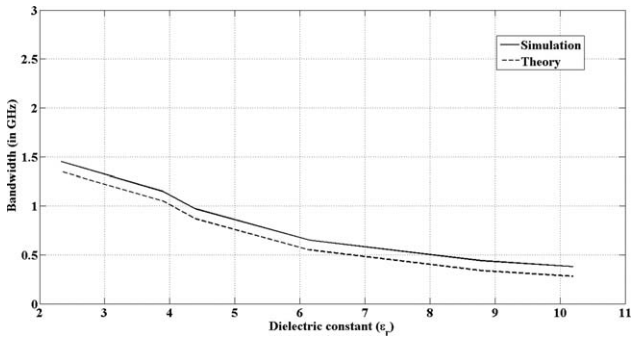

Figure 8 Variation of dielectric constant (ε_r) vs. impedance BW for rectangular PMA

rectangular PMA as shown in Figure 7. Figure 8 shows that impedance BW degrades with the increase in dielectric constant and follows (5) developed in Section 2. Increase in dielectric constant raises surface wave which in turn reduces the radiated power.

4. CONCLUSION

Input impedance of a HED on an ungrounded substrate is first derived using transmission line analogy. We extract the circuit parameters with closed form expressions for resistive and reactive parts for both TE and TM polarization case. Circuit representation for PMA is used to calculate reflection coefficient. The theoretical results for reflection coefficient of rectangular and circular are compared with simulation results obtained using HFSS software. The proposed method is also found to be reasonably accurate for modelling circular PMA. Beside these, the effect of broadening the width of the patch on the impedance BW for rectangular PMA is also shown in Section 3. Impact of dielectric constant of the substrate material on impedance BW is also presented here.

REFERENCES

1. M. Srifi, S. Podilchak, M. Essaaidi, and Y. Antar, Compact disc monopole antennas for current and future ultrawideband (UWB) applications, IEEE Trans Antennas Propag 59 (2011), 4470–4480.
2. J. Liang, C. Chiau, X. Chen, and C. Parini, Study of a printed circular disc monopole antenna for UWB system, IEEE Trans Antennas Propag 53 (2005), 3500–3504.
3. J.R. Panda and R.S. Kshetrimayum, An F shaped printed monopole antenna for dual-band RFID and WLAN applications, Microwave Opt Technol Lett 53 (2011), 1478–1481.
4. J. Kim, T. Yoon, J. Kim, and J. Choi, Design of an ultra-wideband printed monopole antenna using FDTD and genetic algorithm, IEEE Microwave Wireless Compon Lett 15 (2005), 395–397.
5. W. Wu and Y.P. Zhang, Analysis of ultra-wideband printed planar quasimonopole antennas using the theory of characteristics modes, IEEE Antennas Propag Mag 52 (2010), 67–77.
6. C. Laohapensaeng, C. Free, and I. Robertson, Simplified analysis of printed monopole antenna fed by a CPW, Asia-Pac Microw Conf 5 (2005).
7. D.R. Jackson and N.G. Alexopoulos, Gain enhancement methods for printed circuit antennas, IEEE Trans Antennas Propag 33 (1985).
8. J. Liang, C.C. Chiau, X. Chen, and Clive G. Parini, Study of a Printed Circular Disc Monopole Antenna for UWB Systems, IEEE Trans Antennas Propag 53 (2005), 1710–1711.
9. R. Garg, I. Bahl, P. Bhartia, and A. Ittipiboon, Microstrip Antenna Design Handbook, Artech House, Norwood, MA.
10. A.K. Bhattacharjee, S.R. Bhadra Chaudhuri, D.R. Poddar, and S.K. Chowdhury, Equivalence of radiation properties of square and circular microstrip patch antennas, IEEE Trans Antennas Propag 38 (1990), 1710–1711.

CSRR-BASED COMPACT PENTA BAND PRINTED ANTENNA FOR GPS/GSM/ WLAN/WiMAX APPLICATIONS

S. Imaculate Rosaline and Singaravelu Raghavan
Department of Electronics and Communication Engineering, National Institute of Technology (NIT), Tiruchirappalli, Tamilnadu, India;
Corresponding author: imaculaterosaline@gmail.com

Received 23 December 2014

ABSTRACT: *This article describes the design of a compact penta band triangular patch antenna backed by a hexagonal complementary split ring resonator operating in the GPS (1.57 GHz), GSM (1.80 GHz), WLAN (2.4/5 GHz), and WiMAX (3.5 GHz) bands. The antenna has a very compact dimension of 20 × 20 × 1.6 mm^3. Three concentric hexagonal split ring slots in the ground plane yield the uppermost triple bonds (2.45, 3.5, 5.2 GHz) and the two parameterized radiating branches attached to the triangular patch accounts for the two lowermost operating bands (1.57, 1.8 GHz). A prototype of the proposed antenna is fabricated and tested. Simulated and measured results are in good agreement. It has a uniform radiation pattern over all the operating frequencies and a peak gain of 6.3 dBi at 3.5 GHz.* © 2015 Wiley Periodicals, Inc. Microwave Opt Technol Lett 57:1538–1542, 2015; View this article online at wileyonlinelibrary.com. DOI 10.1002/mop.29133

Key words: *GPS; GSM; WLAN; WiMAX; hexagonal complementary split ring resonator*

1. INTRODUCTION

Recent advancement in wireless communication devices such as mobile phones and laptops requires low cost and compact multiband antennas competent with several communication standards. Achieving multiband operation with a single radiating patch is efficient in terms of compactness and cost effectiveness. This can be accomplished using multiple radiating branches [1,2], creating slots in the patch [3], in the ground plane [4], meandering monopoles [5], creating fractal shapes [6], or using metamaterial inspired structures-like split ring resonators [7,8] and complementary split ring resonators (CSRR) [9,10]. Many multiband antennas suitable for various wireless applications such as GSM, DCS, PCS, UMTS, WLAN, and WiMAX are reported in the literature [11–13]. However, they lack compact size and the